Second Ballooning Stability Effect on H-mode Pedestal Scalings

T. Onjun 1), A.H. Kritz 2), G. Bateman 2), A. Pankin 2)

1) Sirindhorn International Institute of Technology, Klong Luang, Pathumthani, Thailand
2) Department of Physics, Lehigh University, Pennsylvania, USA

E-mail: thawatchai@siit.tu.ac.th

Abstract. Models for the prediction of ion and electron pedestal temperatures at the edge of type I ELMy H-mode plasmas are developed. These models are based on theory motivated concepts for pedestal width and pressure gradient. The pedestal pressure gradient is assumed to be limited by high *n* ballooning mode instabilities, where both the first and second stability limits are considered. The effect of the bootstrap current, which reduces the magnetic shear in the steep pressure gradient region at the edge of the H-mode plasma, can result in access to the second stability of ballooning mode. In these pedestal models, the magnetic shear and safety factor are calculated at a radius that is one pedestal width away from separatrix. The predictions of these models are compared with pedestal data for type I ELMy H-mode discharges obtained from the latest public version (version 3.2) in the International Tokamak Physics Activity Edge (ITPA) Pedestal Database. It is found that the pedestal temperature model based on the magnetic and flow shear stabilization yields the best agreement with experimental data (RMSE of 28.2%). For standard H-mode ITER discharges with 15 MA plasma current, predictive analysis yields ion and electron temperatures at the top of the H-mode pedestal in the range from 1.7 to 1.9 keV.

1. Introduction

It is well known that when the plasma heating power increases, plasmas can undergo a spontaneous self-organizing transition from a low confinement mode (L-mode) to a high confinement mode (H-mode). This plasma activity is widely believed to be caused by the generation of a flow shear at the edge of plasma, which is responsible for suppressed turbulence and transport near the edge of plasma. The reduction of transport near the plasma edge results in a narrow sharply-defined region at the edge of the plasma with steep temperature and density gradients, called the pedestal. This pedestal is located near the last closed magnetic flux surface and typically extends over with a width of about 5% of the plasma minor radius. It was found that energy confinement in the H-mode regime of tokamaks strongly depends on the temperature and density at the top of the pedestal [1]. Therefore, it is important in H-mode tokamak plasma studies, especially for the burning plasma experiment such as the International Thermonuclear Experimental Reactor (ITER) [2], to have a reliable prediction for temperatures at the top of the pedestal.

In the previous pedestal study by T. Onjun *et al*. [3], six theory-based pedestal temperature models were developed using different models for the pedestal width together with a ballooning mode pressure gradient limit that is restricted to the first stability of ballooning modes. These models also include the effects of geometry, bootstrap current, and separatrix, leading to a complicated nonlinear behavior. For the best model, the agreement between model's predictions and experimental data for pedestal temperature is about 30.8% RMSE for 533 data points from the International Tokamak Physics Activity Edge (ITPA) Pedestal Database. One weakness of these pedestal temperature models is the assumption that the plasma pedestal is in the first stability regime of ballooning modes.

In this study, six pedestal width models in Refs. [3-8] are modified to include the effect of the second stability limit of ballooning modes. The predictions from these pedestal temperature models are be tested against the latest public version of the pedestal data (Version 3.2) obtained from the ITPA Pedestal Database. This paper is organized in the following way: In Section 2, the pedestal temperature model development is described. In Section 3, the predictions of the pedestal temperature resulting from the models are compared with pedestal temperature experimental data. A simple statistical analysis is used to characterize the agreement of the predictions of each model with experimental data. The development and comparison with experimental data for the pedestal density models are shown in Section 4. In Section 5, conclusions are presented

2. H-Mode Pedestal Temperature Model

Each pedestal temperature model described in Ref. [1] has two parts: a model for the pedestal width (Δ) and a model for the pressure gradient ($\partial p/\partial r$). The pedestal density, n_{ped}, is obtained directly from the experiment or from the pedestal density model described in Section 4. The temperature at the top of the pedestal (T_{ped}) can be estimated as

$$T_{\text{ped}} = \frac{1}{2\, n_{\text{ped}}\, k} \left| \frac{\partial p}{\partial r} \right| \Delta \tag{1}$$

where k is the Boltzmann constant. Six pedestal models were developed based on Eq. (1) in Ref. [3]. These pedestal models are based on (1) the flow shear stabilization width model [$\Delta \propto (\rho R q)^{1/2}$] [3], (2) the magnetic and flow shear stabilization width model [$\Delta \propto \rho s^2$] [4], (3) the normalized poloidal pressure width model [$\Delta \propto R(\beta_{\theta,\text{ped}})^{1/2}$] [5], (4) the diamagnetic stabilization width model [$\Delta \propto \rho^{2/3} R^{1/3}$] [6], (5) the ion orbit loss width model [$\Delta \propto \varepsilon^{1/2} \rho_\theta$] [7], and (6) the two fluid Hall equilibrium width model [$\Delta \propto (1/Z)(A_{\text{H}}/n_{\text{ped}})^{1/2}$] [8]. Note that the constant of proportionality in the pedestal width scaling based the two fluid Hall equilibrium width model in Ref. [8] is varied in this work to improve agreement with experimental data. These six pedestal width models are used in this paper together with an improved pressure gradient model to develop new pedestal temperature models.

For the maximum pressure gradient in the pedestal of type I ELMy H-mode discharges, the pedestal pressure gradient is approximated as the pressure gradient limit of high-n ballooning modes in the short toroidal wavelength limit. The ballooning mode is usually described using the magnetic shear vs. normalized pressure gradient diagram (s-α diagram). Normally, the calculation of ballooning mode stability is complicated, requiring information about the plasma equilibrium and geometry. A number of different codes have been developed for stability analysis, such as HELENA, MISHKA and ELITE. In Ref. [9], stability analyses for JET triangularity scan H-mode discharges were carried out using the HELENA and MISHKA ideal MHD stability codes. For the JET high triangularity discharge 53298, the stability analysis results are shown in fig. 10 in Ref. [9]. Based on results obtained in Ref. [9], the s-α MHD stability diagram with both the first and second stability effects included can be simplified as Fig. 1. This s-α MHD stability diagram leads to an analytic expression for the critical normalized pressure gradient α_c that includes the effect of both the first and second stability of ballooning modes and geometrical effects given by:

$$\alpha_c \equiv -\frac{2\mu_0 R q^2}{B_T^2}\left(\frac{dp}{dr}\right)_c = \alpha_0(s)\left[\frac{1+\kappa_{95}^2\left(1+10\delta_{95}^2\right)}{7}\right]. \tag{2}$$

where μ_0 is the permeability of free space, R is the major radius, q is the safety factor, B_T is the toroidal magnetic field, s is the magnetic shear, κ_{95} and δ_{95} are the elongation and triangularity at the 95% flux surface, and $\alpha_0(s)$ is a function of magnetic shear as

$$\alpha_0(s) = \begin{cases} 3+0.8(s-4) & s>6 \\ 6-3\sqrt{1-\left(\dfrac{6-s}{3}\right)^2} & 6\geq s\geq 3\,. \\ 6 & 3>s \end{cases} \tag{3}$$

Note that in this work, the effect of geometry on the plasma edge stability has a similar form with that used in Ref. [3], but somewhat stronger. The function in Eq. (3) can be understood as the following: for $s > 6$, the equation indicates that the pedestal is in the first stability regime of ballooning modes; for $6 \geq s \geq 3$, the equation represents the regime of a transition from first to second stability of ballooning modes; for $s < 3$, the equation represents a plasma that is in the second stability of ballooning modes, where the pedestal pressure gradient is limited by finite n ballooning mode stability. It should be noted that the effect of the current-driven peeling mode is not considered in this work. In Eq. (3), the bootstrap current and separatrix effects are included through the calculation of magnetic shear as described in Ref. [1]. Note that the magnetic shear in Ref. [3] is calculated as

$$s = s_0\left(1-\frac{c_{bs}b(\upsilon^*,\varepsilon)\alpha_c}{4\sqrt{\varepsilon}}\right), \tag{4}$$

where the multiplier C_{bs} is adjusted to account for the uncertainty of the bootstrap current effect.

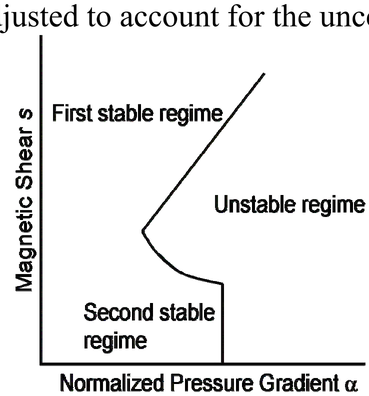

Fig. 1: The normalized pressure gradient vs. magnetic shear diagram (s-α diagram) is plotted. First and second stability region and unstable region is also described.

3. Results and Discussions

Statistical comparisons between predicted pedestal parameters and corresponding experimental values obtained from the ITPA Pedestal Database [10] version 3.2 are carried out. To quantify the comparison between the predictions of each model and experimental data, the root mean-square error (RMSE), the offset, and the Pearson product moment correlation coefficient (R) are computed. The RMSE, offset, and correlation R are defined as

$$\mathrm{RMSE}\ (\%) = 100 \times \sqrt{\frac{1}{N}\sum_{j=1}^{N}\left[\ln\left(T_j^{\exp}\right) - \ln\left(T_j^{\mathrm{mod}}\right)\right]^2}\ ,$$

$$\mathrm{Offset}(\%) = \frac{100}{N}\sum_{j=1}^{N}\left[\ln\left(T_j^{\exp}\right) - \ln\left(T_j^{\mathrm{mod}}\right)\right],$$

$$R = \frac{\sum_{j=1}^{N}\left(\ln\left(T_j^{\exp}\right) - \overline{\ln\left(T_j^{\exp}\right)}\right)\left(\ln\left(T_j^{\mathrm{mod}}\right) - \overline{\ln\left(T_j^{\mathrm{mod}}\right)}\right)}{\sqrt{\sum_{j=1}^{N}\left(\ln\left(T_j^{\exp}\right) - \overline{\ln\left(T_j^{\exp}\right)}\right)^2\left(\ln\left(T_j^{\mathrm{mod}}\right) - \overline{\ln\left(T_j^{\mathrm{mod}}\right)}\right)^2}}$$

where N is total number of data points, and $T_j^{\exp}$ and T_j^{mod} are the j^{th} experimental and model results for the temperature.

Six scalings for the pedestal temperature are derived using the six models described above for the width of the pedestal together with the model given by Eqs. (2) and (3) for the critical pressure gradient that includes both the first and second stability of ballooning modes. The pedestal temperature scalings are calibrated using 457 experimental data points (90 from JET experiment, and 367 from JT-60U experiment) for the ion pedestal temperature from the ITPA Pedestal Database (Version 3.2). The statistical results are shown in Table 1. The value of the coefficient, C_{w}, used in each of the expressions for the pedestal width and the value of multiplier C_{bs} used in the calculation of magnetic shear are given in the second and third column of Table 1, respectively. It is found that the RMSEs for the pedestal temperature range from 28.2% to 109.4%, where the model based on $\Delta \propto \rho s^2$ yields the lowest RMSE. For the offset, it is shown in Table 1 that the offsets range from -6.5% to 9.0%, where the model based on $\Delta \propto \rho s^2$ yields the best agreement (smallest absolute value of the offset). For the correlation R, it is shown in Table 1 that the values of correlation R range from 0.28 to 0.80, where the model based on $\Delta \propto \rho s^2$ yields the best agreement (highest value of R). From these results, it can be concluded that the pedestal temperature based on $\Delta \propto \rho s^2$ yields the best average agreement with experimental data.

Table 1: Statistical results of the models for type 1 ELMy H-mode discharges.

Pedestal width scaling	C_{w}	C_{bs}	RMSE (%)	Offset (%)	R
$\Delta \propto \rho s^2$	5.10	3.0	28.2	0.5	0.80
$\Delta \propto (\rho R q)^{1/2}$	0.22	4.5	35.4	2.9	0.75
$\Delta \propto R(\beta_{\theta,\mathrm{ped}})^{1/2}$	1.50	3.7	35.5	-1.0	0.73
$\Delta \propto \rho^{2/3} R^{1/3}$	1.37	4.9	49.3	-1.1	0.67
$\Delta \propto \varepsilon^{1/2} \rho_\theta$	2.75	4.9	109.4	9.0	0.28
$\Delta \propto (1/Z)(A_{\mathrm{H}}/n_{\mathrm{ped}})^{1/2}$	0.014	5.9	50.5	-6.5	0.68

The comparisons between the predictions of the models and experimental data are shown in Figs. 2-7. It can be seen that the predictions of pedestal temperature are in reasonable agreement with experimental data for the model with $\Delta \propto \rho s^2$ shown in Fig. 2 and the agreement is not as good for the other models shown in Figs. 3-7.

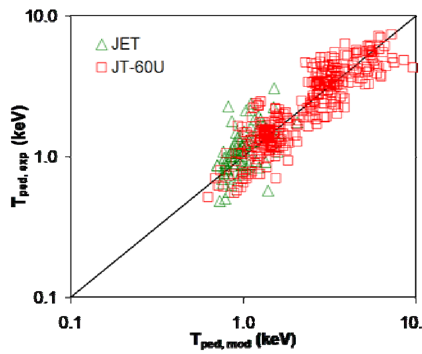

Fig. 2: Experimental ion pedestal temperature for type I H-mode plasmas compared with the model predictions based on $\Delta \propto \rho s^2$.

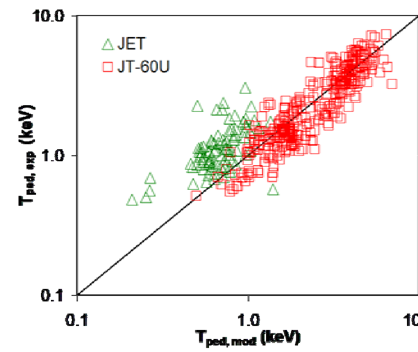

Fig. 3: Experimental ion pedestal temperature for type I H-mode plasmas compared with the model predictions based on $\Delta \propto (\rho R q)^{1/2}$.

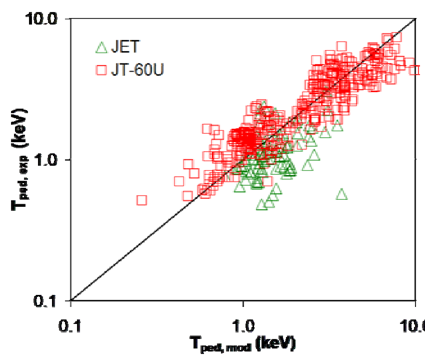

Fig. 4: Experimental ion pedestal temperature for type I H-mode plasmas compared with the model predictions based on $\Delta \propto R(\beta_{\theta,\mathrm{ped}})^{1/2}$.

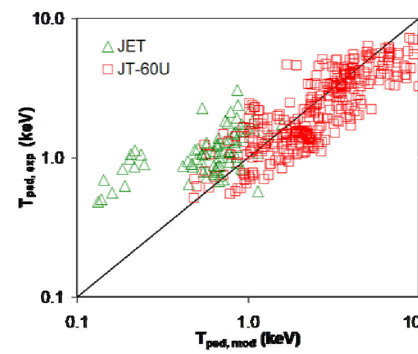

Fig. 5: Experimental ion pedestal temperature for type I H-mode plasmas compared with the model predictions based on $\Delta \propto \rho^{2/3} R^{1/3}$.

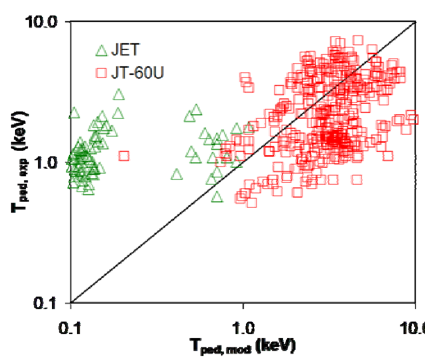

Fig. 6: Experimental ion pedestal temperature for type I H-mode plasmas compared with the model predictions based on $\Delta \propto \varepsilon^{1/2} \rho_\theta$.

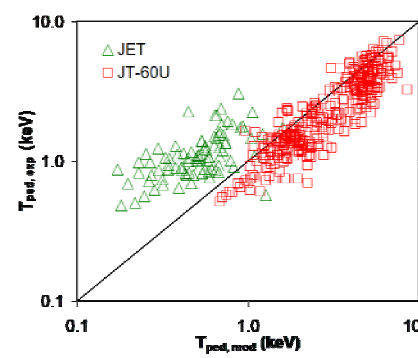

Fig. 7: Experimental ion pedestal temperature for type I H-mode plasmas compared with the model predictions based on $\Delta \propto (1/Z)(A_H/n_{ped})^{1/2}$.

4. H-Mode Pedestal Density Model

In the development of the pedestal density model, an empirical approach is employed. For the simplest scaling, the pedestal density is assumed to be a function of line average density (n_l). This assumption is based on an observation that the density profile between the pedestal and the magnetic axis in H-mode discharges is usually rather flat. Therefore, the pedestal density is a large fraction of the line average density. It is found that the pedestal density scaling for type I ELMy H-mode discharges is about 72% of the line average density, which can be described as

$$n_{\mathrm{ped}} = 0.72 n_l \,. \tag{5}$$

This scaling yields an RMSE of 12.2%, R^2 of 0.96, and offset of -2.2% with a data set of 626 data points (132 from ASDEX-U experiment, 127 from JET experiment, and 367 from JT-60U experiment). In Ref. [11], a pedestal density scaling is developed for Alcator CMOD H-mode discharges. This scaling is expressed as a function of the line average density, plasma current (I_p), and toroidal magnetic field (B_T). Using this kind of power law regression fit for the 626 data points in the ITPA Pedestal Database (Version 3.2), the best predictive pedestal density scaling for type I ELMy H-mode discharges is found to be

$$n_{\mathrm{ped}}\left[10^{20}\,\mathrm{m}^{-3}\right] = 0.74\left(n_{\mathrm{l}}\left[10^{20}\,\mathrm{m}^{-3}\right]\right)^{0.99}\left(I_{\mathrm{p}}\left[MA\right]\right)^{0.15}\left(B_{\mathrm{T}}\left[T\right]\right)^{-0.12} . \tag{6}$$

This scaling yields an RMSE of 10.9%, R^2 of 0.97, and offset of 3.3%. The comparisons of the density models' predictions for the pedestal density using Eq. (5) and (6) and the experimental data are shown in Figs. 8 and 9, respectively. In both figures, the agreement is good for a low ratio of pedestal density to the Greenwald density. However, the agreement tends to break away at high density. This might indicate that the physics that controls low and high edge density might be different.

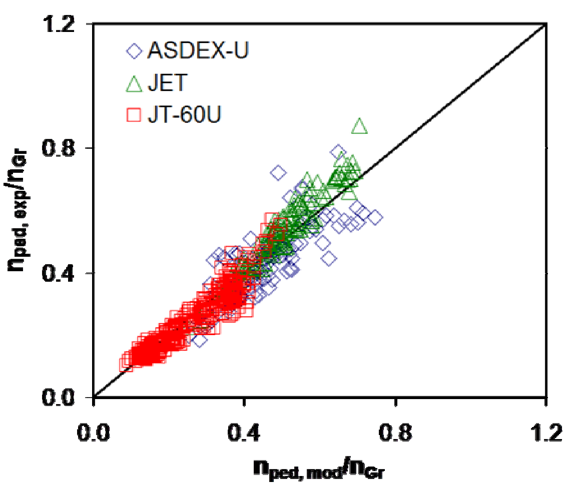

Fig. 8: The ratios of experimental pedestal electron density for type I H-mode plasmas to the Greenwald density are compared with the ratio of the model predictions using Eq. (5) to the Greenwald density.

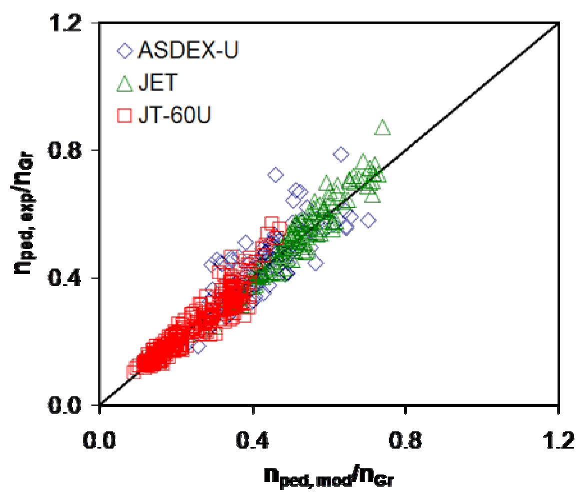

Fig. 9: The ratios of experimental pedestal electron density for type I H-mode plasmas to the Greenwald density are compared with the ratio of the model predictions using Eq. (6) to the Greenwald density.

5. Pedestal Prediction in ITER

The pedestal temperature and density models developed in this paper are used to predict the pedestal parameters for the ITER design. For an ITER standard H-mode discharge with 15 MA plasma current and the line average density of 1.05×10^{20} particles/m^3, the pedestal density is predicted to be 0.76×10^{20} particles/m^3 and 0.95 $\times 10^{20}$ particles/m^3 using Eqs. (5) and (6), respectively. It is worth noting that the pedestal density using Eq.(6) indicate a flat density profile since the pedestal density is almost the same as the line average density. This observation is often observed in H-mode experiments with high density. In addition, the pedestal density in ITER predicted using an integrated modeling code JETTO yields similar result for the density profile [12]. The pedestal temperature model based on the width of the pedestal as $\Delta \propto \rho s^2$ and the critical pressure gradient model that includes both first and second stability of ballooning modes is used to predict the pedestal temperature in ITER. Figure 10 shows the predicted pedestal temperature as a function of pedestal density. It can be seen that the pedestal temperature decreases as the pedestal density increases. At the predicted pedestal density using Eqs. (5) and (6), the predicted pedestal temperature is 1.9 and 1.7, respectively. Under these conditions, it is found that the pedestal width in ITER predicted by the model ranges from 4 to 5 cm.

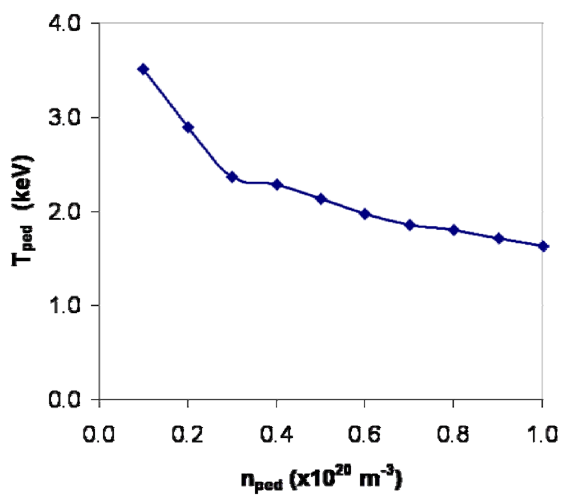

Fig. 10: Predictions of pedestal temperature as a function of pedestal density using the pedestal temperature model based on $\Delta \propto \rho s^2$

6. Conclusions

Pedestal temperature models that include the effects of both the first and second stability of ballooning modes are developed for type I ELMy H-mode plasmas in tokamaks. The results for the pedestal temperature are compared with experimental data obtained from the ITPA Pedestal Database version 3.2. It is found that the pedestal temperature model based on the magnetic and flow shear stabilization yields the best agreement with experimental data (with RMSE of 28.2%). It is found that the predictions of pedestal temperatures for ITER using the pedestal temperature and density models developed ranges from 1.7 to 1.9 keV.

4. Acknowleagement

Authors are grateful to Prof. Suthat Yoksan for his helpful discussions and to the ITPA Pedestal Database group for the pedestal data used in this work. This work is partially supported by Commission on Higher Education and the Thailand Research Fund (TRF) under Contract No. MRG4880165.

5. Referecnes

[1] Kinsey J E *et al.*, 2003 *Nucl. Fusion* **43** 1845
[2] Aymar R *et al.*, 2002 *Plasma Phys. Control. Fusion* **44** 519
[3] Onjun T *et al.,* 2002 *Phys. Plasmas* **9** 5018
[4] M Sugihara *et al.,* 2000 *Nucl. Fusion* **40** 1743
[5] T H Osborne *et al.,* 1999 *J. Nucl. Mater*. **266–269** 131
[6] B N Rogers *et al.*, 1999 *Phys. Plasmas* **6** 2797
[7] K C Shaing, 1992 *Phys. Fluids B* **4** 290
[8] Guzdar P N *et al.,* 2005 *Physics of Plasmas* **12** 032502
[9] Onjun T *et al.*, 2004 *Phys. Plasmas* **11** 3006
[10] Hatae T *et al.,* 2001 *Nucl. Fusion* **41** 285
[11] Hughes J W *et al.,* 2002 *Physics of Plasmas* **9** 3019
[12] Onjun T *et al.,* 2005 *Physics of Plasmas* **12** 082513